



Configuration-interaction calculations on the $3s^23p^n$ configuration of neutral phosphorus and two of its ions

Adnan Yousif Hussein ^{*}*College of Education, Mustansiriyah University, Baghdad 46219, Iraq* (Received 17 July 2021; revised 4 November 2021; accepted 21 December 2021; published 12 January 2022)

We perform valence, core-core, and core-valence nonrelativistic configuration-interaction (CI) calculations on the states belonging to the $3s^23p^n$ configuration with $n = 2, 3$, and 4, for P^+ ($^3P, ^1D, ^1S$), P ($^4S^\circ, ^2D^\circ, ^2P^\circ$), and P^- ($^3P, ^1D, ^1S$) species, respectively. Excitation energies, ionization potential, and electron affinities related to these states were calculated using orbital basis sets up to $\ell = 12$ and corrected with relativistic contributions. We also carry out relativistic CI calculations for the fine structure splitting of the sublevels $^3P_{0,1,2}$ and $^3P_{2,1,0}$ in P^+ and P^- , respectively, and both $^2D_{3/2,5/2}^\circ$ and $^2P_{1/2,3/2}^\circ$ in P , using orbital basis sets up to $\ell = 3$. Systematic studies on the convergence of both nonrelativistic and relativistic CI calculations for each electronic state show the energy contributions corresponding to each CI excitation level. Our results for the excitation energies, ionization potential, and electron affinity of the $(3s^23p^3)^4S^\circ$ ground state, as well as fine structure splittings, are in very good agreement with the experiment and give reliability to the predicted electron affinities of the $(3s^23p^3)^2D^\circ$ and $^2P^\circ$ excited states of 1135(1) meV and 1040(1) meV, respectively.

DOI: [10.1103/PhysRevA.105.012809](https://doi.org/10.1103/PhysRevA.105.012809)

I. INTRODUCTION

In contrast to neutral atoms and cations, anions have only a limited number of stable states. These states are often correspond to ground states which are energetically below the ground states of the parent neutral atom. On the other hand, there are metastable states of anions with relatively long lifetimes which are energetically above the ground states of the neutral parent atom and lie below the continuum with the same LS symmetry and parity [1]. Often such metastable states are corresponding to excited discrete states. Most of the stable states can be identified to a certain accuracy with different *ab initio* methods, e.g., the Hartree-Fock (HF), multiconfiguration Hartree-Fock (MCHF), configuration interaction (CI), and other many-body techniques. Extra care should be exercised with metastable states for reasons outlined below.

In addition to the fact that metastable states are difficult to observe experimentally, theoretical work on metastable states or even stable ones of the anion involves many difficulties not encountered in the corresponding neutral and cations states. One of the main difficulties is often the ability of the significant electron-electron interaction to change the electronic orbitals upon the binding of an additional electron to the neutral atom. Furthermore, the wave function expansion grows too rapidly with each step toward incorporating configurations from higher excitation levels. Another source of difficulty is the diffusion of the spatial extent of the outermost orbitals, and this in turn requires an extra linear combination of primitive functions to represent the atomic orbitals. Despite high CPU time and slow convergence of radial expansion problems in

the CI method, both nonrelativistic and relativistic CI regimes fall within the realm of one of the most accurate *ab initio* methods for it to offer a clear way to define a systematic approach. In the present paper, we will employ the CI method to calculate the energy levels of $^4S^\circ, ^2D^\circ$, and $^2P^\circ$ states of the neutral phosphorus, $P(3s^23p^3)$, and the $^3P, ^1D$, and 1S states in both $P^+(3s^23p^2)$ and $P^-(3s^23p^4)$ ions. The importance of studying P comes from its relative abundance, and it is regarded as an indicator of possible life in other parts of the universe [2]. P^+ is of particular interest because it has a silicon-like electronic configuration. The spectra of P^+ and P are well known experimentally [3–6] and calculated at a certain level of accuracy [7,8]. On the other hand, the $(3s^23p^4)^3P$ ground bound state in P^- is well observed experimentally. The electron affinity (EA) of the $(3s^23p^3)^4S^\circ$ ground state was first reported by Andersson *et al.* [9] to 746.68(6) meV, and then it was updated to be 746.607(10) meV by Peláez *et al.* [10]. Theoretically, many studies using a variety of traditional quantum chemical methods have been done to predict the binding energy of the 3P ground stable state [11–14]. The landmark *ab initio* and density functional calculations augmented with core-valence contribution done by de Oliveira [15] predicted the EA of the $^4S^\circ$ ground state to 742.64 meV, which agrees well with the experiment. However, the difference between the de Oliveira *et al.* result and the experiment is more than 4 meV. On the other hand, an early investigation carried out by Bunge *et al.* [16] revealed the existence of both excited metastable $(3s^23p^4)^1D$ and 1S states against autoionization. Their work, however, does not give explicit numerical values of the binding energies of these states with respect to $(3s^23p^3)^2D^\circ$ and $^2P^\circ$ parent states, respectively. The metastable 1D and 1S states are formed from the corresponding excited neutral parents $^2D^\circ$ and $^2P^\circ$ states, respectively. However, it should be mentioned that the formation of the 3P state could readily

*adnanyousif@uomustansiriyah.edu.iq

be observed, and no indication of the formation of the 1D and 1S states has been found in any of the experiments carried out so far [10]. In an LS-coupling scheme, the 1D term cannot autoionize to the continuum of the bound $^4S^\circ$ term of the neutral P. Likewise, the 1S term cannot autoionize to the continua associated with either the $^4S^\circ$ or $^2D^\circ$ term. The autoionization becomes possible only when the magnetic interactions are taken into account. However, radiative transitions by an electric dipole without spin change are allowed into lower bound [17–21] or continuum [22,23] states including resonances [24].

The purpose of this paper is to calculate excitation energy (EE), ionization potential (IP), and EA related to P^+ (3P , 1D , and 1S), P ($^4S^\circ$, $^2D^\circ$, and $^2P^\circ$), and P^- (3P , 1D , and 1S). Furthermore, the fine structure splitting of the neutral and ionic states of P are calculated within the framework of relativistic CI up to an excitation level equal to the number of valence electrons outside an inactive core. Predictions of EE, IP, and EA require calculation of energy differences between the corresponding states; one may define an inactive core and consider only the correlation among the valence electrons. However, including core-core and core-valence correlation is crucial to achieve accurate predictions of atomic properties with respect to the corresponding experimental data.

In Sec. II we review the main features of nonrelativistic CI method including the generation of configuration lists, and the construction of the CI wave function for valence, core-core, and core-valence correlations. We also describe the procedure to obtain energy-optimized atomic orbitals to within prescribed accuracy starting from a small set of primitive functions. In Sec. III we give a summary of the theoretical background of the employed relativistic CI method. In Sec. IV we summarize and discuss the numerical results of the different correlation energy contributions and the corresponding EEs, IP, EAs, and fine structure splitting. Finally, Sec. V gives concluding remarks.

II. THE NONRELATIVISTIC CALCULATIONS

Three sets of nonrelativistic CI calculations are reported in the present paper. One set concerns the valence correlation energies of the 3P , 1D , and 1S terms in both P^+ ($3s^23p^2$) and P^- ($3s^23p^4$), and $^4S^\circ$, $^2D^\circ$, and $^2P^\circ$ terms in P ($3s^23p^3$). The other two sets of CI calculations concern both core-core and core-valence correlation energy contributions.

A. The CI wave function

In the nonrelativistic CI method, the wave function Ψ_μ of an atomic bound state labeled μ can be expressed as a linear combination of configuration state functions (CSFs) F_{gK} with total quantum numbers L , M_L , S , M_S (in the LS coupling scheme) and of the same parity

$$\Psi_\mu = \sum_{K=1}^{K_x} \sum_{g=1}^{g_K} F_{gK} C_{gK}, \quad (1)$$

where K and g labels are for configuration and degenerate element, respectively, and K_x and g_K keep track of the highest values. K and g , respectively, and C_{gK} are expansion coeffi-

icients. Each CSF is obtained upon application of a symmetric projection operator $O(\Gamma, \gamma)$ [25] for all pertinent symmetry operators Γ and a given irreducible representation γ , as successively orthogonalized symmetric projections of Slater determinants; i.e., F_{gK} may be expressed as linear combination of n_K Slater determinants D_{iK} ,

$$F_{gK} = O(\Gamma, \gamma) \sum_{i=1}^g D_{iK} b_i^g = \sum_{i=1}^{n_K} D_{iK} c_i^g. \quad (2)$$

The program AUTOCL [26–28] was used to generate all CSFs associated with single (S), double (D), triple (T), quadruple (Q), quintuple (Qn), and sextuple (Se) electron excitation from a given single or multireference configuration. The full CI (FCI) space of an atomic state can be achieved by including all CSFs generated from S -, D -, T -excitations, etc., up to a maximum number of electrons in the system within reasonably one electron basis set representation. When the CI wave function includes CSFs restricted to excitations from valence orbitals, we define the valence (VV) correlation model. If the CI wave function includes CSFs limited to excitations from core orbitals, we define the core-core (CC) correlation model. The remaining correlation is the core-valence (CV) correlation model, which covers CSFs created by excitations from combination of both core and valence orbitals, with the restriction of allowing at most five holes in the core at the SD excitation level. It is noteworthy that CC excitations generate much larger configurations lists than the corresponding VV and CV excitations. In the nonrelativistic CI approach, Schrödinger's equation can be written in matrix form, in terms of a column vector of expansion coefficients \mathbf{C}_μ , an interaction matrix \mathbf{H} , and the variational upper bound FCI energy E_μ^{FCI} ,

$$\mathbf{H}\mathbf{C}_\mu = E_\mu^{\text{FCI}}\mathbf{C}_\mu. \quad (3)$$

The nonrelativistic energy E_μ^{nr} (exact eigenvalue of Schrödinger's equation) is related to E_μ^{FCI} through the relation [29],

$$E_\mu^{\text{nr}} = E_\mu^{\text{FCI}} + \Delta E_\mu^{\text{OBI}} + \Delta E_\mu^{\text{CI}}, \quad (4)$$

where $\Delta E_\mu^{\text{OBI}}$ is the error due to orbital basis incompleteness [17,30], and ΔE_μ^{CI} represents the truncation energy error due to any simplification to the FCI computation effected in the evaluation of E_μ^{nr} . Calculation of FCI energy even with a small system is computationally intractable due to the vast number of the CI size, which increases progressively with higher excitation levels. Therefore, the CI space should be reduced in some way, and hopefully both the approximate CI wave function and the corresponding CI energy are as close as possible to the exact values. To manage large CI expansions, we use the following procedure. First, *a priori* selected CI (SCI) with truncation energy error [31] takes place to reduce the CI size; however, the outcome CI space may still be huge for direct CI and needs to be further truncated into a selected space (S -space). Second, the program ATMOL [32] has the ability to perform CI by parts (CIBP) [33,34] in which the S -space is partitioned into several subspaces ($S_0, S_1, S_2, \dots, S_r$) of dimensions ($d_0, d_1, d_2, \dots, d_r$), respectively. Here S_0 is the reference space in which all

CI coefficients are always variational, and all other subspaces S_i , $i = 1, 2, \dots, r$ will be taken up variationally one after the other. The theoretical basis of *a priori* SCI with truncation energy error and CIBP has been widely discussed elsewhere [31,33,34], and we will not go into its details here.

B. Orbital basis set

In this work, the radial part $R_{n\ell}$ of the one electron wave function is chosen to be a linear combination of energy-optimized Slater-type orbitals (STOs),

$$R_{n\ell}(r) = \sum_k a_{nk\ell} \frac{(2\xi_{k\ell})^{(n_{k\ell}+1/2)}}{[(2n_{k\ell})!]^{1/2}} r^{(n_{k\ell}-1)} e^{-r\xi_{k\ell}}, \quad (5)$$

where n and ℓ are the principal quantum number and the orbital quantum number, respectively. The parameters $a_{nk\ell}$ and $\xi_{k\ell}$ in Eq. (5) are the orbital expansion coefficients and the nonlinear parameter orbital exponent, respectively. For each irreducible representation (irrep) of LS symmetry, a new STO is introduced in the form of a set of trial primitives (N_t). N_t optimization processes are dispatched simultaneously, where orbital exponents within a given irrep are reoptimized in the sense to obtain the lowest energy for single or multireference CISD. The choice of the primitive STOs for given atomic orbitals and a given state plays a crucial role later in all CI convergence stages for VV, CC, and CV calculations. In the VV calculation of both P^+ (3P , 1D , and 1S) and P ($^4S^\circ$, $^2D^\circ$, and $^2P^\circ$), we started by approximating the occupied orbitals, $1s$, $2s$, and $3s$ by ten STOs of s -type, and both $2p$ and $3p$ orbitals by eight STOs of p -type, and set up to satisfy the HF energy [35] of the considered state. For P^- (3P , 1D , and 1S), the initial orbital basis are augmented with additional reoptimized six STOs of d -type, four STOs of f -type, and two STOs of g -type, to describe the diffuse charge of the negative ion states. Thereafter, the orbital space of VV wave function is extended to include all CSFs at SD excitations outside the neon fixed core up to the orbital harmonic $\ell = 12$, where the orbital basis are automatically optimized until saturation is reached within a prescribed threshold of energy decrements (cutoff = $5 \mu\text{hartree}$); one can reach reasonable convergence for a certain type of orbital symmetry. It is important to point out that only CSFs interacting directly with their corresponding reference configuration (HF configuration) are retained in the CISD level during automatic optimization. These ‘‘HF interacting spaces’’ [36] yield the largest contributions to the correlation energy and furthermore reduce CPU time for automatic optimization. These composite energy-optimized STO basis sets were eventually used to compute the corresponding variational upper bound valence energies up to CISDTQ, CISDTQQn, and CISDTQQnSe for P^+ (3P , 1D and 1S), P ($^4S^\circ$, $^2D^\circ$, and $^2P^\circ$), and P^- (3P , 1D , and 1S), respectively. Likewise, both CC and CV calculations employed the same initial orbital STO representation of VV calculations except that automatic optimization run over CSFs belonging to configuration lists of CC and CV. In this investigation, we maintain systematic proceeding of the calculation in which each excitation level incorporates the same maximum number of virtual orbitals for each species. Table I presents the number of energy-optimized STOs per each orbital symmetry (column 4) for each term (column 2) of P^+ , P , and P^- species (column 1). According

to Table I, the CC correlation calculation displays the largest number of STOs among both VV and CV correlation.

One of the methods to assess the quality of the wave functions is the analysis of the angular energy pattern of convergence, which provides prior simulation of the quality of the energy-optimized STOs and consequently the final form of the total wave function. We do not report here the tables that display the pattern of convergence. However, our study on the CISD energy of VV contribution with increasing angular momentum up to $\ell=12$ for 3P , 1D , and 1S terms of P^+ shows that the angular energy pattern of the excited 1S term is the most rapid convergence among 3P and 1D terms. Therefore, energy optimization for the 1S term is finished with 68 STOs, while it takes 73 and 77 additionally built STOs for 3P and 1D terms, respectively, as indicated in Table I. On the other hand, the angular energy pattern of both CC and CV contributions of the same terms are much slower than that of the VV contribution, and this reflect the larger number of STOs basis for both CC and CV calculations. Vice versa, in VV calculation of P , the excited $^2P^\circ$ term exhibited the slowest angular energy convergence pattern with respect to both $^4S^\circ$ and $^2D^\circ$ terms. When going to both CC and CV correlation calculations, the excited $^2P^\circ$ term shows instabilities upon STOs automatic optimization. The instabilities of angular energy convergence can be attributed to the choice of the initial STOs basis. However, if we change or modify our initial basis of one-electron orbitals, we observe that at a certain level of precision, the resulted basis set suffers approximate linear dependence instead. For P^- , the pattern of the 3P term displays the most rapid energy convergence with respect to the pattern of both the 1D and 1S term; however, the 1S term has the smallest CISD size among both 3P and 1D terms. The effect of truncation of the virtual VV, CC, and CV correlation space represented by orbital basis incompleteness (column 6) is obtained as an extrapolation of the last eight values of the nonrelativistic CISD energy up to $\ell = 400$, as a function of the angular momentum of the energy functional,

$$\Delta E(\ell) = \sum_i [E_i(\ell) - E_i^{\text{patt}}(\ell)]^2, \quad (6)$$

where $E_i^{\text{patt}}(\ell)$ is based on Schwartz’s law [37] and $E_i^{\text{patt}}(\ell) = a_o(\ell + \delta)^{-4}$, in which a_o and δ are adjustable parameters.

III. THE RELATIVISTIC CALCULATIONS

Detailed accounts of the relativistic CI method have been discussed by Bunge and coworkers [38–40], and we will mention only the outline of the method. The starting point for N -particle relativistic calculations is the combination of one-electron Dirac Hamiltonian h_D and electron-electron interaction V_{ij} ,

$$H = \sum_{i=1}^N h_D(i) + \sum_{i>j}^N V_{ij}. \quad (7)$$

For an electron moving in Coulomb potential of stationary-point nucleus of charge Z , h_D (in atomic units) is then

$$h_D = c\boldsymbol{\alpha} \cdot \mathbf{p} + (\beta - 1)c^2 - \frac{Z}{r}. \quad (8)$$

TABLE I. STO basis sets per orbital symmetry, total number of STOs, and the corresponding orbital basis incompleteness error (in μ hartrees) of various correlation calculations at CISD approximation for P^+ (3P , 1D , and 1S), P ($4S^\circ$, $2D^\circ$, and $2P^\circ$), and P^- (3P , 1D , and 1S).

Species	Term	Correlation	STOs set	No. of STOs	ΔE^{OBI}
P^+	3P	VV	12s 12p 8d 8f 6g 5h 5i 4k 4l 3m 2n 2o 2q	73	-45
		CC	16s 15p 13p 12f 10g 10h 9i 8k 7l 5m 5n 4o 3q	117	-76
		CV	14s 13p 11d 10f 9g 8h 6i 6k 5l 3m 2n 1o 1q	89	-40
	1D	VV	12s 12p 8d 8f 7g 5h 5i 5k 4l 4m 3n 2o 2q	77	-46
		CC	16s 16p 13d 13f 11q 10h 9i 8k 7l 5m 5n 4o 3q	120	-81
		CV	14s 13p 11d 10f 9g 7h 6i 6k 5l 3m 2n 1o 1q	88	-44
	1S	VV	12s 11p 8d 6f 6g 5h 5i 4k 3l 3m 2n 2o 1q	68	-41
		CC	11s 13p 14d 9f 8g 7h 7i 7k 5l 5m 5n 4o 3q	98	-93
		CV	11s 12p 10d 8f 7g 6h 6i 3k 3l 2m 1n 1o 1q	71	-53
P	$4S^\circ$	VV	12s 12p 9d 8f 7g 6h 5i 5k 4l 4m 3n 2o 2q	79	-70
		CC	15s 15p 13d 12f 10g 10h 9i 8k 7l 5m 5n 4o 3q	116	-98
		CV	14s 14p 12d 10f 9g 8h 7i 6k 5l 3m 3n 1o 1q	93	-91
	$2D^\circ$	VV	13s 12p 10d 8f 7g 6h 6i 5k 5l 4m 4n 3o 2q	85	-83
		CC	15s 15p 13d 12f 10q 10h 9i 8k 6l 5m 5n 4o 3q	115	-75
		CV	13s 13p 12d 10f 9g 8h 7i 6k 5l 3m 3n 1o 1q	91	-81
	$2P^\circ$	VV	11s 12p 11d 10f 7g 6h 6i 6k 5l 5m 4n 3o 2q	88	-87
		CC	9s 11p 12d 9f 4q 3h 2i 2k 1l 1m 1n 1o 1q	57	-81
		CV	10s 11p 12d 11f 7q 6h 5i 3k 3l 1m 1n 1o 1q	72	-96
P^-	3P	VV	12s 12p 11d 8f 7g 7h 6i 6k 5l 5m 4n 3o 3q	89	-125
		CC	13s 15p 13d 12f 10g 10h 9i 8k 6l 5m 5n 4o 3q	113	-103
		CV	11s 13p 12d 10f 9g 8h 7i 6k 5l 3m 3n 1o 1q	89	-89
	1D	VV	13s 13p 10d 9f 7g 7h 6i 6k 5l 5m 4n 4o 3q	92	-111
		CC	15s 17p 12d 13f 11g 10h 9i 8k 7l 5m 5n 4o 3q	119	-127
		CV	12s 14p 13d 10f 9g 8h 7i 6k 5l 3m 3n 1o 1q	92	-76
	1S	VV	13s 13p 11d 9f 7g 7h 7i 6k 5l 5m 4n 4o 3q	94	-116
		CC	11s 14p 11d 10f 9g 9h 7i 7k 6l 5m 5n 4o 3q	101	-97
		CV	11s 13p 12d 11f 9g 8h 7i 6k 5l 3m 2n 1o 1q	89	-66

In fully relativistic theory, Breit interaction is the most important correction; therefore, V_{ij} in Eq. (7) can be modified as the sum of the usual Coulomb electron-electron repulsion r_{ij}^{-1} and Breit interaction B_{ij} . In our work the latter is treated via variational calculation,

$$V_{ij} = r_{ij}^{-1} + B_{ij}, \quad (9)$$

$$B_{ij} = -\frac{1}{2} \left(\frac{\vec{\alpha}_i \cdot \vec{\alpha}_j}{r_{ij}} + \frac{(\vec{\alpha}_i \cdot \vec{r}_{ij})(\vec{\alpha}_j \cdot \vec{r}_{ij})}{r_{ij}^3} \right). \quad (10)$$

The basis of the one-electron wave function known as the double primitive (DP) basis can be defined as normalized Dirac bispinors [41] embracing $2m$ -dimensional n_{ir} irreducible representations,

$$\phi_{n\ell j m_j}^{(i+m)} = \frac{1}{r} \begin{pmatrix} P_{n\ell j}(r) \mathcal{Y}_{\kappa m_j} \\ -i Q_{n\ell j}(r) \mathcal{Y}_{-\kappa m_j} \end{pmatrix}, \quad i = 1, 2, \dots, i_x(\ell j), \quad (11)$$

$$m = \sum_{(\ell j)}^{n_{\text{ir}}} i_x(\ell j), \quad (12)$$

where $P_{n\ell j}(r)$ and $Q_{n\ell j}(r)$ are the upper and lower components of the radial wave function, respectively, and $\mathcal{Y}_{\kappa m_j}$ is the usual spherical spinor in the $\ell s j$ coupling scheme. In order to set up a counterpart CI wave function suitable for relativis-

tic calculations, CSF is taken to be an eigenfunction of the total angular momentum J^2 with eigenvalue $\hbar^2 J(J+1)$, expressed as a linear combination of Slater determinants, which in turn is composed of DP basis. Hence one could obtain equations similar to Eqs. (1) and (2), in jj-JM rather than LS-coupling. Representation of Eq. (7) in terms of finite-size DP basis yields an eigenvalue problem of dimension $\mathcal{N}(2m)$ corresponding to complete spectrum of H , i.e., including both positive $\mathcal{N}^+(m)$ and negative-energy $\mathcal{N}^-(m)$ N -particle states,

$$\mathbf{H}\mathbf{C}_i = E_i \mathbf{C}_i, \quad i = 1, 2, \dots, \mathcal{N}(2m). \quad (13)$$

Let us denote the matrix of the no-pair Hamiltonian [42,43] with \mathbf{H}^+ of dimension $\mathcal{N}^+(m)$, and the corresponding energy with E_i^+ . The difference between the dimensions of \mathbf{H} and \mathbf{H}^+ is defined as $\mathcal{N}^-(m)$,

$$\mathcal{N}^-(m) = \mathcal{N}(2m) - \mathcal{N}^+(m). \quad (14)$$

The interleaving theorem [44] for finite-size Hermitian matrices yields the corollary,

$$E_i^+ \leq E_{i+\mathcal{N}^-}, \quad i = 1, 2, \dots, \mathcal{N}^+. \quad (15)$$

Hence, the eigenvalues $E_{i+\mathcal{N}^-}$ of the full and invariant representation of \mathbf{H} are an upper bound to the eigenvalues E_i^+ of the

TABLE II. LS terms of $P^+(3s^23p^2)$, $P(3s^23p^3)$, and $P^-(3s^23p^4)$ species expressed in terms of jj -configuration, number of negative and positive-energy states, target eigenvalue, and STO basis sets per orbital symmetry.

Species	Term	J	Configuration	\mathcal{N}^-	\mathcal{N}^+	Target eigenvalue	STO set	
P^+	3P	0	$(3s^23p^2 + 3s^23P^2)$	6643	1932	$\mathcal{N}^- + 1$	11s 9p 9P 7d 7D 5f 5F	
		1	$(3s^23p3P)$	8710	2509	$\mathcal{N}^- + 1$	11s 9p 9P 7d 7D 5f 5F	
		2	$(3s^23P^2 + 3s^23p3P)$	11 446	3391	$\mathcal{N}^- + 1$	11s 9p 9P 7d 7D 5f 5F	
	1D	2	$(3s^23P^2 + 3s^23p3P)$	11 446	3391	$\mathcal{N}^- + 2$	11s 9p 9P 7d 7D 5f 5F	
		1S	0	$(3s^23p^2 + 3s^23P^2)$	6643	1932	$\mathcal{N}^- + 2$	11s 9p 9P 7d 7D 5f 5F
P	$^4S^\circ$	3/2	$(3s^23P^3 + 3s^23p3P^2 + 3s^23p^23P)$	31 105	8949	$\mathcal{N}^- + 1$	11s 9p 9P 7d 7D 5f 5F	
		$^2D^\circ$	3/2	$(3s^23P^3 + 3s^23p3P^2 + 3s^23p^23P)$	31 105	8949	$\mathcal{N}^- + 2$	11s 9p 9P 7d 7D 5f 5F
		5/2	$(3s^23p3P^2)$	11 886	3459	$\mathcal{N}^- + 1$	11s 9p 9P 7d 7D 5f 5F	
	$^2P^\circ$	1/2	$(3s^23p3P^2)$	11 117	3247	$\mathcal{N}^- + 1$	11s 9p 9P 7d 7D 5f 5F	
		3/2	$(3s^23P^3 + 3s^23p3P^2 + 3s^23p^23P)$	31 105	8949	$\mathcal{N}^- + 3$	11s 9p 9P 7d 7D 5f 5F	
P^-	3P	2	$(3s^23p^23P^2 + 3s^23p3P^3)$	48 990	14 101	$\mathcal{N}^- + 1$	9s 9p 9P 7d 7D 6f 6F	
		1	$(3s^23p3P^3)$	13 263	3855	$\mathcal{N}^- + 1$	9s 9p 9P 7d 7D 6f 6F	
		0	$(3s^23P^4 + 3s^23p^23P^2)$	14 500	4179	$\mathcal{N}^- + 1$	9s 9p 9P 7d 7D 6f 6F	
	1D	2	$(3s^23p^23P^2 + 3s^23p3P^3)$	48 990	14 101	$\mathcal{N}^- + 2$	9s 9p 9P 7d 7D 6f 6F	
	1S	0	$(3s^23P^4 + 3s^23p^23P^2)$	14 500	4179	$\mathcal{N}^- + 2$	9s 9p 9P 7d 7D 6f 6F	

corresponding no-pair Hamiltonian \mathbf{H}^+ . Thus, Eq. (13) can be rewritten as a sets of the two-eigenvalue problem,

$$\mathbf{H}\mathbf{C}_j = E_j\mathbf{C}_j, \quad j = 1, 2, \dots, \mathcal{N}^-, \quad (16)$$

$$\mathbf{H}\mathbf{C}_{\mathcal{N}^-+i} = E_{\mathcal{N}^-+i}\mathbf{C}_{\mathcal{N}^-+i}, \quad i = 1, 2, \dots, \mathcal{N}^+. \quad (17)$$

Solutions of Eq. (17) are stable upon any variations. Thus, only after jumping over the lower \mathcal{N}^- eigensolutions of Eq. (16) do we find a genuine variational theorem valid for the remaining higher-lying eigenvalues encompassing the ground and all excited eigenstates, all of them with positive energies $E_{\mathcal{N}^-+i}$ which are an upper bounds to the eigenvalues E_i^+ . In nonrelativistic calculations, the HF wave function is made up of a single LS-coupling configuration. However, in relativistic calculations the wave function should be jj -coupling. Thus, a linear combination of several jj -coupling configurations may be required to represent a single LS-coupling configuration. In this work, the upper component of the radial functions $P_{n\ell j}$ of the Dirac bispinor is chosen to be a linear combination of generalized Dirac-STOs [34],

$$P_{n\ell j}(r) = \sum_k a_{nk\ell j} r^{(\gamma+n\ell j-1)} e^{(-\xi_{k\ell j}r)}, \quad (18)$$

where $\gamma = [\kappa^2 - (\alpha Z)^2]^{1/2} \geq \frac{1}{2}$, *viz.*, $Z \leq 118$, and both $a_{nk\ell j}$ and $\xi_{k\ell j}$ are taken from the corresponding STO basis optimized up to $\ell = 3$ at the nonrelativistic SD excitation level. The generalized Dirac-STO basis set is used to extract positive-energy natural orbitals at the valence relativistic CISD level of approximation. Later we use this to perform relativistic CI valence calculation up to the SDTQ(QnSe) level of approximation. Table II displays the jj -multireference configuration for the states under consideration, number of negative and positive-energy states, target eigenvalue, and the number of STOs per each orbital symmetry. For instance, the present basis set (11s 9p 9P 7d 7D 5f 5F) of the sub-level $J = 0$ belongs to the 3P term of P^+ , yields $\mathcal{N}^+ = 1932$ positive-energy state, and $\mathcal{N}^- = 6643$ negative-energy state; thus the first (ground) bound state is the target eigenvalue

of order 6644. The second (first excited) bound $J = 0$ state corresponding to the 1S term is the target eigenvalue of order 6645. In Table II upper and lower case letters are for $j = \ell + 1/2$ and $j = \ell - 1/2$ orbitals, respectively. Note that the reported calculations use point nucleus and speed of light $c = 137.03599976(50)$.

IV. RESULTS AND DISCUSSION

A. Excitation energies of the 1D and 1S states of $P^+(3s^23p^2)$

In Table III we list different contributions of nonrelativistic CI energies of VV, CC, and CV, in addition to relativistic differential energy contribution (ΔR) for the states 3P , 1D , and 1S of $P^+(3s^23p^2)$. The contributions to the excitation energies $EE(^1D-^3P)$ and $EE(^1S-^3P)$ are illustrated with systematically increasing of excitation level up to SDTQ. The results of numerical HF [45] are added up for comparison with our corresponding finite basis set HF. At the Hartree-Fock level of approximation, a large discrepancy is seen between theory and experiment of 2440 cm^{-1} and 6295 cm^{-1} for $EE(^1D_0-^3P_0)$ and $EE(^1S_0-^3P_0)$, respectively. As seen in Table III, more and more VV correlation is included progressively when going from the SD to SDTQ excitation level. The nonrelativistic CI energy given in Eq. (4) has been estimated at the SDTQ level for VV calculation, lying both 1D and 1S at $8622(1) \text{ cm}^{-1}$ and $21\,341(1) \text{ cm}^{-1}$, respectively, with respect to 3P . However, VV calculations still yield EEs less than the experiment by roughly 250 cm^{-1} and 230 cm^{-1} for both $EE(^1D-^3P)$ and $EE(^1S-^3P)$, respectively. The differential CI energy contributions of both CC and CV correlations have been estimated as the difference between the nonrelativistic CI energies for each of SD, SDT, and SDTQ levels with respect to the HF energy associated with each term. As shown in Table III, the CC correlation contributions are negative for $EE(^1D-^3P)$, i.e., smaller EE, and positive for $EE(^1S-^3P)$. When going from SD up to the SDTQ excitation level, the CC contribution exhibited maximum change of -7 cm^{-1} and 31 cm^{-1} for both $EE(^1D-^3P)$ and $EE(^1S-^3P)$, respectively. In contrast to CC

TABLE III. Nonrelativistic CI energy contributions of VV correlation, differential CI energy contributions of both CC and CV correlations, and differential relativistic CI energy contributions ΔR (in hartrees) of 3P , 1D , and 1S states in $P^+(3s^23p^2)$, with systematic increase of excitation level, and the corresponding excitation energies, EE (in cm^{-1}).

Correlation	Approximation	3P	1D	1S	EE(1D - 3P)	EE(1S - 3P)
VV	HF	-340.349774114	-340.298188461	-340.222785416	11 321.742	27 870.798
	Numerical HF	-340.34977577	-340.29818989	-340.22278732	11 321.792	27 870.743
	CISD	-340.443810825	-340.404301644	-340.346649834	8671.263	21 324.373
	CISDT	-340.445339411	-340.406026918	-340.347664765	8628.095	21 437.107
	CISDTQ	-340.445514965	-340.406228859	-340.348281107	8622.304	21 340.365
	E^{nr}	-340.445560108	-340.406275202	-340.348322129	8622(1)	21 341(1)
CC ^a	CISD	-0.378087333	-0.378520785	-0.377675691	-95.132	90.345
	CISDT	-0.378618889	-0.379068289	-0.378310773	-98.632	67.623
	CISDTQ	-0.378866810	-0.379324425	-0.378571553	-100.435	64.801
	ΔE_{cc}^{nr}	-0.378943023	-0.379405786	-0.378664580	-102(3)	61(3)
CV ^a	CISD	-0.049340124	-0.049188872	-0.048909855	33.196	94.433
	CISDT	-0.049509987	-0.049398745	-0.049121165	24.415	85.337
	CISDTQ	-0.049595021	-0.049517326	-0.049248040	17.052	76.154
	ΔE_{cv}^{nr}	-0.049635152	-0.049561428	-0.049301554	16(2)	73(2)
ΔR	DHF ^a	-0.847706925	-0.846109348	-0.844137207	350.628	783.463
	CISD ^b	-0.847438232	-0.846304000	-0.846324147	248.935	244.513
	CISDT ^c	-0.847923331	-0.846362427	-0.847398365	342.579	115.217
	CISDTQ ^d	-0.847923575	-0.846357118	-0.847458477	343.798	102.077
	ΔE^r	-0.847923575	-0.846357118	-0.847458477	344(3)	102(3)
Predicted				8880(9)	21 577(9)	
Experiment ^e				8882.31	21 575.63	

^aThe corresponding energies can be calculated by adding the respective HF energy.

^bThe corresponding energies can be calculated by adding the respective nonrelativistic CISD energy.

^cThe corresponding energies can be calculated by adding the respective nonrelativistic CISDT energy.

^dThe corresponding energies can be calculated by adding the respective nonrelativistic CISDTQ energy.

^eRef. [5].

correlation, the CV correlation shows positive contributions to both EE(1D - 3P) and EE(1S - 3P). Moreover, when going from SD up to SDTQ excitation, both EE(1D - 3P) and EE(1S - 3P) display a maximum change of 17 cm^{-1} and 21 cm^{-1} , respectively. However, both CC and CV contributions to each of EE(1D - 3P) and EE(1S - 3P) show a decrease with respect to the excitation level. The extrapolated nonrelativistic energy limit for CC and CV have been estimated, and the corresponding differential energy contributions are labeled as ΔE_{cc}^{nr} and ΔE_{cv}^{nr} , respectively. Even with CC and CV contributions taken into account, the nonrelativistic theory is not always sufficient to achieve better agreement with the experiment. Relativistic effects are expected to be rigorous. According to spectroscopic data [5], the term 3P has two states with $J = 1$ and $J = 2$ that appear, respectively, at 164.90 cm^{-1} and 469.12 cm^{-1} above that with $J = 0$, so that $J = 0$, the lowest state, defines the reference state of $P^+(3s^23p^2)$. The ΔR , are obtained as the difference between relativistic CI valence energy and the corresponding nonrelativistic CI energy calculated at the valence level of approximation. For instance, the result of ΔR at CISD level of calculation of the 3P state is obtained as the difference between the relativistic CISD valence energy of the lowest level ($J = 0$) calculated with a basis set of $11s\ 9p\ 9P\ 7d\ 7D\ 5f\ 5F$ and the corresponding nonrelativistic CISD of VV calculation with a basis set of $11s\ 9p\ 7d\ 5f$. The term DHF represents the differential energy contribution of

the self-consistent multireference Dirac-Hartree-Fock, while the term ΔE^r represents the relativistic correction up to higher excitation level of the valence calculation rounded to zero decimal places. The predicted EEs were obtained by adding both final differential contributions ΔE_{cc}^{nr} and ΔE_{cv}^{nr} of CC and CV, respectively, as well as ΔE^r , together with the corresponding VV energy contribution. The predicted EE(1D - 3P) and EE(1S - 3P) became 8880(9) cm^{-1} and 21 577(9) cm^{-1} , respectively, which are in excellent agreement with the most accurate experimental data of Martin *et al.* [5]. The estimated accuracy are given within parentheses.

B. Excitation energies of the $^2D^\circ$ and $^2P^\circ$ states of $P(3s^23p^3)$

As in Table III, in Table IV we summarize our calculated CI energies for $^4S^\circ$, $^2D^\circ$, and $^2P^\circ$ states in $P(3s^23p^3)$, and their corresponding contributions to both EE($^2D^\circ$ - $^4S^\circ$) and EE($^2P^\circ$ - $^4S^\circ$). In VV calculations, both EE($^2D^\circ$ - $^4S^\circ$) and EE($^2P^\circ$ - $^4S^\circ$) have their maximum contributions at SD excitation level and gradually decreases toward SDTQn excitation. The EE($^2D^\circ$ - $^4S^\circ$) obtained at the VV level up to SDTQn is 11 365(1) cm^{-1} and shows satisfactory agreement with experiment. However, the calculated EE($^2P^\circ$ - $^4S^\circ$) is less than the experiment by 95 cm^{-1} . The effect of both CC and CV correlation display a negative contribution to EE($^2D^\circ$ - $^4S^\circ$) and stabilized at -59(4) cm^{-1} and -49(2) cm^{-1} , respectively. Similarly, the CC and CV contributions to EE($^2P^\circ$ - $^4S^\circ$) are

TABLE IV. Nonrelativistic CI energy contributions of VV correlation, differential CI energy contributions of both CC and CV correlations, and differential relativistic CI energy contributions ΔR (in hartrees) of $^4S^\circ$, $^2D^\circ$, and $^2P^\circ$ states in $P(3s^23p^3)$, with systematic increase of excitation level, and the corresponding excitation energies, EE (in cm^{-1}).

Correlation	Approximation	$^4S^\circ$	$^2D^\circ$	$^2P^\circ$	EE($^2D^\circ$ - $^4S^\circ$)	EE($^2P^\circ$ - $^4S^\circ$)
VV	HF	-340.718780588	-340.648869576	-340.603301824	15 343.694	25 344.659
	Numerical HF	-340.71878085	-340.64887043	-340.60330382	15 343.564	25 344.278
	CISD	-340.826970375	-340.774336028	-340.740120132	11 551.904	19 061.425
	CISDT	-340.831390261	-340.779299893	-340.744941758	11 432.514	18 973.253
	CISDTQ	-340.831994253	-340.780185239	-340.746848963	11 370.764	18 687.231
	CISDTQQn	-340.832008259	-340.780211300	-340.747128608	11 368.118	18 628.930
	E^{nr}	-340.832078624	-340.780295051	-340.747216046	11 365(1)	18 625(1)
CC ^a	CISD	-0.376229512	-0.376935749	-0.376793435	-155.001	-123.767
	CISDT	-0.376933709	-0.377379020	-0.377415769	-97.734	-105.800
	CISDTQ	-0.377208282	-0.377520488	-0.377606662	-68.521	-87.434
	CISDTQQn	-0.377264530	-0.377554242	-0.377641641	-63.584	-82.766
	ΔE_{cc}^{nr}	-0.377363268	-0.377629745	-0.377723003	-59(4)	-79(4)
CV ^a	CISD	-0.050367037	-0.050726900	-0.049786446	-78.981	127.425
	CISDT	-0.050554944	-0.050866979	-0.050343270	-68.484	46.457
	CISDTQ	-0.050669276	-0.050917503	-0.050607488	-54.480	13.561
	CISDTQQn	-0.050711237	-0.050944327	-0.050660931	-51.157	11.041
	ΔE_{cv}^{nr}	-0.050803073	-0.051025809	-0.050757502	-49(2)	10(2)
ΔR	DHF ^a	-0.846078551	-0.846301510	-0.846604041	-48.934	-115.332
	CISD ^b	-0.846579024	-0.847005531	-0.845318022	-93.607	276.758
	CISDT ^c	-0.846702841	-0.847045774	-0.845817755	-75.265	194.254
	CISDTQ ^d	-0.846748580	-0.846285642	-0.8459345406	101.603	178.661
	CISDTQQn ^e	-0.846754407	-0.846281076	-0.846005969	103.884	164.263
	ΔE^r	-0.846754407	-0.846281076	-0.846005969	104(3)	164(3)
Predicted				11 361(10)	18 720(10)	
Experiment ^f				11 361.02	18 722.71	

^aThe corresponding energies can be calculated by adding the respective HF energy.

^bThe corresponding energies can be calculated by adding the respective nonrelativistic CISD energy.

^cThe corresponding energies can be calculated by adding the respective nonrelativistic CISDT energy.

^dThe corresponding energies can be calculated by adding the respective nonrelativistic CISDTQ energy.

^eThe corresponding energies can be calculated by adding the respective nonrelativistic CISDTQQn energy.

^fRef. [5].

stabilized at $-79(4) \text{ cm}^{-1}$ and $10(2) \text{ cm}^{-1}$, respectively. The contribution of relativistic effect ΔR is taken between the lowest $^2D_{3/2}^\circ$ and $^2P_{1/2}^\circ$ sublevels with respect to $^4S_{3/2}^\circ$. A final relativistic correction ΔE^r is obtained at CISDTQQn level of positive contributions of $104(3) \text{ cm}^{-1}$ and $164(3) \text{ cm}^{-1}$ to both $\text{EE}(^2D^\circ - ^4S^\circ)$ and $\text{EE}(^2P^\circ - ^4S^\circ)$, respectively. When CC and CV contributions and ΔE^r are added together to the VV calculations, the predicted $\text{EE}(^2D^\circ - ^4S^\circ)$ and $\text{EE}(^2P^\circ - ^4S^\circ)$ are $11\,361(10) \text{ cm}^{-1}$ and $18\,720(10) \text{ cm}^{-1}$, respectively, which are both in excellent agreement with the experiment.

C. Ionization potential and electron affinity of the $(3s^23p^3)^4S^\circ$ ground state

In Table V we listed the results of the $(3s^23p^2)^3P$ state in Table III and $(3s^23p^3)^4S^\circ$ state in Table IV together with the corresponding CI energy contributions of $(3s^23p^4)^3P$ state. Table V also displays our calculated ionization potential $\text{IP}(^3P-^4S^\circ)$ and electron affinity $\text{EA}(^4S^\circ-^3P)$ of $(3s^23p^3)^4S^\circ$ ground state at different excitation levels. These are compared with best previous calculated results of ionization

potential of Koga *et al.* [46] and electron affinity of de Oliveira *et al.* [15], as well as the corresponding experimental data [3,10]. The VV calculation exhibits very good convergence to about 1 meV for the last two excitation levels of both IP and EA, leading to excellent prediction of EA of $748.0(1) \text{ meV}$ at CISDTQQn(Se) with respect to the experimental value of $746.607(10) \text{ meV}$ [10]. However, the calculated IP is $10\,517.8(1) \text{ meV}$, still higher than experiment by 31 meV. On the other hand, inclusion of CC contribution reduces the calculated IP and EA at all excitation levels leading to $-43.0(4) \text{ meV}$ and $-25.0(4) \text{ meV}$, respectively, at SDTQ(QnSe). In contrast to CC, the contribution of CV is positive and leads to $32.0(3) \text{ meV}$ and $18.0(3) \text{ meV}$ at CISDTQ(QnSe) for IP and EA, respectively. The relativistic correction to IP shows a negative contribution at all excitation levels up to CISDTQ(Qn). In contrast to IP, the relativistic correction to EA, varies between negative and positive and then becomes stable at a relatively small value of 2 meV. The predicted IP and EA are $10\,474.8(9) \text{ meV}$ and $743.0(9) \text{ meV}$, in very good agreement with respect to experiment of $10\,486.77(03) \text{ meV}$ [3] and $746.607(10) \text{ meV}$ [10], respectively.

TABLE V. Nonrelativistic CI energy contributions of VV correlation, differential CI energy contributions of both CC and CV correlations, and differential relativistic CI energy contributions ΔR (in hartrees) of $(3s^23p^2)^3P$, $(3s^23p^3)^4S^\circ$, and $(3s^23p^4)^3P$ states, with systematic increase of excitation level, and the corresponding ionization potential IP (in meV) and ground state electron affinity EA (in meV).

Correlation	Approximation	$E(^3P)$	$E(^4S^\circ)$	$E(^3P)$	IP(3P - $^4S^\circ$)	EA($^4S^\circ$ - 3P)
VV	HF	-340.349774114	-340.718780588	-340.698650006	10 041.182	-547.781
	Numerical HF	-340.34977577	-340.71878085	-340.69887346	10 041.144	-541.708
	CISD	-340.443810825	-340.826970375	-340.845827722	10 426.307	513.135
	CISDT	-340.445339411	-340.831390261	-340.855476153	10 504.984	655.411
	CISDTQ	-340.445514965	-340.831994253	-340.859275751	10 516.642	742.368
	CISDTQ(Qn)		-340.832008259	-340.859418690	10 517.023	745.876
	CISDTQ(QnSe)			-340.859440643		746.474
	E^{nr}	-340.445560108	-340.832078624	-340.859565884	10 517.8(1)	748.0(1)
CC ^a	CISD	-0.378087333	-0.376229512	-0.375143837	-50.554	-29.542
	CISDT	-0.378618889	-0.376933709	-0.375914241	-45.856	-27.741
	CISDTQ	-0.378866810	-0.377208282	-0.376133862	-45.131	-29.236
	CISDTQ(Qn)		-0.377264530	-0.376247235	-43.600	-27.682
	CISDTQ(QnSe)			-0.376332409		-25.364
	ΔE_{cc}^{nr}	-0.378943023	-0.377363268	-0.376435633	-43.0(5)	-25.0(5)
CV ^a	CISD	-0.049340125	-0.050367037	-0.051038683	27.944	18.276
	CISDT	-0.049509987	-0.050554944	-0.051193026	28.435	17.363
	CISDTQ	-0.049595021	-0.050669276	-0.051227633	29.232	15.193
	CISDTQ(Qn)		-0.050711237	-0.051344730	30.373	17.238
	CISDTQ(QnSe)			-0.051373141		18.011
	ΔE_{cv}^{nr}	-0.049635152	-0.050803073	-0.051462368	32.0(3)	18.0(3)
ΔR	DHF ^a	-0.847706925	-0.846078551	-0.846201214	-56.373	3.338
	CISD ^b	-0.847438232	-0.846579024	-0.846122736	-23.380	-12.416
	CISDT ^c	-0.847923331	-0.846702841	-0.846123580	-33.211	-15.763
	CISDTQ ^d	-0.847923575	-0.846748580	-0.846584197	-31.973	-4.473
	CISDTQ(Qn) ^e		-0.846754407	-0.846796078	-31.815	1.134
	CISDTQ(QnSe) ^f			-0.846822653		1.857
	ΔE^r	-0.847923575	-0.846754407	-0.846822653	-32.0(4)	2.0(4)
Predicted				10 475(1)	743(1)	
Best previous calculation				9989.92 ^g	742.64 ^h	
Experiment				10 486.77(03) ⁱ	746.607(10) ^j	

^aThe corresponding energies can be calculated by adding the respective HF energy.

^bThe corresponding energies can be calculated by adding the respective nonrelativistic CISD energy.

^cThe corresponding energies can be calculated by adding the respective nonrelativistic CISDT energy.

^dThe corresponding energies can be calculated by adding the respective nonrelativistic CISDTQ energy.

^eThe corresponding energies can be calculated by adding the respective nonrelativistic CISDTQn energy.

^fThe corresponding energies can be calculated by adding the respective nonrelativistic CISDTQnSe energy.

^gRef. [46].

^hRef. [15].

ⁱRef. [3].

^jRef. [10].

D. Electron affinities of the $(3s^23p^3)^2D^\circ$ and $2P^\circ$ excited states

Table VI displays different energy contributions of both $2D^\circ$ and $2P^\circ$ states of $P(3s^23p^3)$, and both $1D$ and $1S$ states of $P^-(3s^23p^4)$ together with the corresponding electron affinities EA($2D^\circ$ - $1D$) and EA($2P^\circ$ - $1S$) at different levels of excitation. As seen in Table VI, EA($2P^\circ$ - $1S$) is negative at HF level, corresponding to unbound $1S$ state in contrast to the corresponding numerical HF result. A positive EA($2P^\circ$ - $1S$) is first obtained after inclusion of SD excitation. A further significant increase of energy contribution of VV with excitation level up to SDTQn(Se) gives the crucial contribution to both EA($2D^\circ$ - $1D$) and EA($2P^\circ$ - $1S$). In general, both CC and CV

contributions exhibit relatively slow change (increasing or decreasing) of electron affinities of both $2D^\circ$ and $2P^\circ$ states with respect to the SDTQ through SDTQnSe excitation level. The relativistic correction at CISDTQnSe displays a relatively large negative contribution of $-238.0(4)$ meV for EA($2D^\circ$ - $1D$) with respect to $-33.5(4)$ meV for EA($2P^\circ$ - $1S$). The predicted values of both EA($2D^\circ$ - $1D$) and EA($2P^\circ$ - $1S$) are 1135(1) meV and 1040(1) meV, respectively. In the present case, where no experimental data are known, we can reveal that the binding energy of the $1D_2$ excited state is 1016 meV above the ground state $3P_2$, and the $1S_{1/2}$ excited state is located 1007 meV above the $1D_2$ excited state.

TABLE VI. Nonrelativistic CI energy contributions of VV correlation, differential CI energy contributions of both CC and CV correlations, and differential relativistic CI energy contributions ΔR (in hartrees) for $(3s^2 3p^3)^2 D^\circ$, $^2 P^\circ$ states, and $(3s^2 3p^4)^1 D$, $^1 S$ states, with systematic increase of excitation level, and the corresponding excited state electron affinities, EA¹ and EA² (in meV).

Correlation	Approximation	E(² D [°])	E(² P [°])	E(¹ D)	E(¹ S)	EA ¹	EA ²	
VV	HF	-340.648869576	-340.603301824	-340.659749579	-340.603233726	296.060	-1.853	
	Numerical HF	-340.64887043	-340.60330382	-340.66006740	-340.60349728	304.685	52.643	
	CISD	-340.774336028	-340.740120132	-340.814800809	-340.774044288	1101.103	923.124	
	CISDT	-340.779299893	-340.744941758	-340.824770512	-340.779976422	1237.319	953.342	
	CISDTQ	-340.780185239	-340.746848963	-340.828950102	-340.786034078	1326.960	1066.282	
	CISDTQQn	-340.780211300	-340.747128608	-340.829005947	-340.786754545	1327.770	1078.277	
	CISDTQQn(Se)	<i>E^{nr}</i>	-340.780295051	-340.747216046	-340.829141879	-340.786921063	1329.2(1)	1080.4(1)
CC ^a	CISD	-0.376935749	-0.376793435	-0.376853906	-0.375985644	-2.227	-21.981	
	CISDT	-0.377379020	-0.377415769	-0.377537615	-0.376473787	4.316	-25.632	
	CISDTQ	-0.377520488	-0.377606662	-0.378391374	-0.376756455	23.698	-23.135	
	CISDTQQn	-0.377554242	-0.377641641	-0.378427581	-0.376788536	23.765	-23.214	
	CISDTQQn(Se)	ΔE_{cc}^{nr}	-0.377629745	-0.377723003	-0.378613647	-0.376925051	26.7(5)	-21.7(5)
	CV ^a	CISD	-0.050726900	-0.049786446	-0.050972071	-0.050885907	6.971	29.918
CV ^a	CISDT	-0.050866979	-0.050343270	-0.051311212	-0.051051725	12.088	19.278	
	CISDTQ	-0.050917503	-0.050607488	-0.051480618	-0.051187943	15.323	15.794	
	CISDTQQn	-0.050944327	-0.050660931	-0.051555620	-0.051198447	16.634	14.626	
	CISDTQQn(Se)	ΔE_{cv}^{nr}	-0.051025809	-0.050757502	-0.051646260	-0.051223770	17.019	15.315
	ΔR	DHF ^a	-0.846301510	-0.846601796	-0.868107335	-0.922849652	593.367	2074.750
	ΔR	CISD ^b	-0.847005531	-0.845318022	-0.841594253	-0.839103908	-147.248	-169.095
CISDT ^c		-0.847045774	-0.845817755	-0.840893652	-0.845758157	-167.408	-1.622	
CISDTQ ^d		-0.846285642	-0.845934541	-0.837570909	-0.844628673	-237.140	-35.534	
CISDTQQn ^e		-0.846281076	-0.846005969	-0.837548285	-0.844853856	-237.631	-31.351	
CISDTQQn(Se) ^f		ΔE^r	-0.846281076	-0.846005969	-0.837542819	-0.844813203	-237.780	-32.457
Predicted						-238.0(4)	-33.5(4)	
						1135(1)	1040(1)	

¹EA(²D[°]-¹D).

²EA(²P[°]-¹S).

^aThe corresponding energies can be calculated by adding the respective HF energy.

^bThe corresponding energies can be calculated by adding the respective nonrelativistic CISD energy.

^cThe corresponding energies can be calculated by adding the respective nonrelativistic CISDT energy.

^dThe corresponding energies can be calculated by adding the respective nonrelativistic CISDTQ energy.

^eThe corresponding energies can be calculated by adding the respective nonrelativistic CISDTQQn energy.

^fThe corresponding energies can be calculated by adding the respective CISDTQQnSe energy.

E. Theoretical fine structure splittings

In Table VII we present our relativistic energies calculated at DHF approximation and at relativistic CI valence

approximation up to SDTQ excitation level for the sublevels ³P_{0,1,2} in P⁺(3s²3p²). Furthermore, Breit contributions are analyzed by including the operator variationally. We compare

TABLE VII. Relativistic energies (in hartrees) of the sublevels ³P_{0,1,2} in P⁺(3s²3p²), with systematic increase of excitation level, and the corresponding fine structure splitting ΔJ (in cm⁻¹).

Approximation	E(J = 0)	E(J = 1)	E(J = 2)	$\Delta J_{1,0}$	$\Delta J_{2,0}$
DHF	-341.197481039	-341.197085457	-341.195599653	86.82	412.92
CISD	-341.287603133	-341.286543254	-341.285718071	232.62	413.72
CISDT	-341.289471841	-341.288649775	-341.287229339	180.42	492.17
CISDTQ	-341.289559479	-341.288737178	-341.287316834	180.47	492.20
CISDTQ+Breit	-341.219668830	-341.218886815	-341.217546699	171.63	465.75
Experiment ^a				164.90	469.12

^aRef. [5].

TABLE VIII. Relativistic energies (in hartrees) of the sublevels ${}^2D_{3/2,5/2}^\circ$ and ${}^2P_{1/2,3/2}^\circ$ in $P(3s^23p^3)$, with systematic increase of excitation level, and the corresponding fine structure splittings ΔJ (in cm^{-1}).

Approximation	$J = 3/2$	$J = 5/2$	$\Delta J_{5/2,3/2}$
DHF	-341.495171086	-341.494887831	62.17
CISD	-341.612778199	-341.612081768	152.85
CISDT	-341.617048799	-341.616872385	38.72
CISDTQ	-341.617808217	-341.617722722	18.76
CISDTQQn	-341.617817149	-341.617734542	18.13
CISDTQQn+Breit	-341.547967285	-341.547896814	15.47
Experiment ^a			15.61
Approximation	$J = 1/2$	$J = 3/2$	$\Delta J_{3/2,1/2}$
DHF	-341.449905865	-341.450033352	
CISD	-341.578378798	-341.579973022	
CISDT	-341.584405053	-341.584490415	
CISDTQ	-341.585884655	-341.585692469	42.18
CISDQQn	-341.585912613	-341.585792008	26.47
CISDTQQn+Breit	-341.516063827	-341.515956683	23.52
Experiment ^a			25.3

^aRef. [5].

the calculated fine structure splitting $\Delta J_{1,0}$ (column 5) and $\Delta J_{2,0}$ (column 6) with the available measurements [5]. Our calculated relativistic CI energies up to CISDTQ without Breit interaction corrections give fine structure splitting agreeing with the experimental results within 91% to 95% for $\Delta J_{1,0}$ and $\Delta J_{2,0}$, respectively. In general, the inclusion of the Breit contribution often raises the total absolute energy. However, inclusion of Breit interaction shifts the agreement up to 96% and 99% for both $\Delta J_{1,0}$ and $\Delta J_{2,0}$, respectively.

Table VIII reports in two blocks the relativistic CI valence energies up to the CISDTQQn excitation level for the sublevels ${}^2D_{3/2,5/2}^\circ$ and ${}^2P_{1/2,3/2}^\circ$, in $P(3s^23p^3)$, together with the corresponding fine structure splitting $\Delta J_{5/2,3/2}$ and $\Delta J_{3/2,1/2}$, respectively. In the upper half of Table VIII, we compare our calculated $\Delta J_{5/2,3/2}$ of ${}^2D_{3/2,5/2}^\circ$ with the experiment. A maximum reduction of the calculated $\Delta J_{5/2,3/2}$ toward convergence with the experiment occurs when triple excitations included in the configuration list yield a reduction of 132 cm^{-1} with respect to CISD. Also, inclusion of quadruple excitation represents the crucial effect to converge with the experiment. Inclusion of the Breit interaction contribution at CISDTQQn approximation yields 15.47 cm^{-1} , which is in excellent agreement with experiment. The second half of Table VIII displays the corresponding results for ${}^2P_{1/2,3/2}^\circ$. Results of $\Delta J_{3/2,1/2}$ calculated at DHF up to the CISDT level of approximation display negative values (blank lines) illustrating the difficulty of getting reliable relativistic CI results for fine structure splittings at low excitation level of valence approximation. In contrast to ${}^2D_{3/2,5/2}^\circ$, inclusion of quintuple excitation to the relativistic CI valence calculation of ${}^2P_{1/2,3/2}^\circ$, shows the crucial effect to $\Delta J_{3/2,1/2}$, leading to very good agreement of 26.47 cm^{-1} with respect to experiment of 25.3 cm^{-1} [5]. Unfortunately, this agreement is slightly broken when including Breit interaction, which reduces $\Delta J_{3/2,1/2}$ by about 3 cm^{-1} .

Table IX shows the relativistic CI valence energies of $J = 2, 1$, and 0 levels belonging to the 3P ground term of $P^-(3s^23p^4)$, and the corresponding fine structure splittings

$\Delta J_{1,2}$ and $\Delta J_{0,2}$, calculated at different levels of approximation from DHF through CI up to the SDTQQnSe excitation level. As seen from Table IX, there is systematic reduction of both $\Delta J_{1,2}$ and $\Delta J_{0,2}$ contributions with the excitation level. Our calculated relativistic CI valence energies up to CISDTQQnSe without Breit interaction corrections give fine structure splittings that agree with the experiment [10] within 91% to 98% for $\Delta J_{1,2}$ and $\Delta J_{0,2}$, respectively. However, inclusion of Breit interaction shifted the agreement to 95% and 97% for both $\Delta J_{1,2}$ and $\Delta J_{0,2}$, respectively.

V. SUMMARY AND CONCLUSIONS

We report on valence, core-core, and core-valence non-relativistic CI calculations as well as relativistic CI valence calculations, and their contributions to excitation energies, ionization potential, and electron affinities of both ground and excited states related to ${}^4S^\circ$, ${}^2D^\circ$, and ${}^2P^\circ$ states of neutral phosphorus, $P(3s^23p^3)$, and the 3P , 1D , and 1S states in both $P^+(3s^23p^2)$ and $P^-(3s^23p^4)$ ions. Furthermore, the fine structure splittings of the $(3s^23p^2)^3P_{0,1,2}$ sublevel in P^+ , $(3s^23p^3)^2D_{3/2,5/2}^\circ$, and ${}^2P_{1/2,3/2}^\circ$ sublevels in P and $(3s^23p^4)^3P_{2,1,0}$ sublevel in P^- are calculated within the framework of relativistic CI valence approximation. The present paper provides explicit data for the contribution of valence, core-core, and core-valence in addition to relativistic effects as a function of excitation level. Core-core together with core-valence shows how much more demanding such calculations are even though the effect from the core is dominant. Our calculated excitation energies and ionization potential are in very good agreement with the available experimental data. Furthermore, the excellence of our predicted ground state electron affinity as well as the fine structure splitting with their corresponding experimental data provides motivation to accept the validity of the predicted electron affinities of both ${}^2D^\circ$ and ${}^2P^\circ$ excited states in $P(3s^23p^3)$.

TABLE IX. Relativistic energies (in hartrees) of the sublevels $^3P_{2,1,0}$ in $P^-(3s^23p^3)$, with systematic increase of excitation level, and the corresponding fine structure splitting (in cm^{-1}).

Approximation	$E(J = 2)$	$E(J = 1)$	$E(J = 0)$	$\Delta J_{1,2}$	$\Delta J_{0,2}$
DHF	-341.544851220	-341.544120350	-341.543990343	160.47	188.94
CISD	-341.682067533	-341.680780605	-341.680707464	282.45	298.50
CISDT	-341.690135046	-341.688970875	-341.688936705	255.51	263.01
CISDTQ	-341.693068985	-341.691963874	-341.691889874	242.54	258.79
CISDTQQn	-341.693142287	-341.692146043	-341.691981194	218.65	254.83
CISDTQQnSe	-341.693228645	-341.692317970	-341.692001315	197.68	269.37
CISDTQQnSe+Breit	-341.623347419	-341.622479036	-341.622182637	190.58	255.64
Experiment ^a				181(2)	263(2)

^aRef. [10].

- [1] P. Feldman and R. Novick, *Phys. Rev.* **160**, 143 (1967).
- [2] B.-C. Koo, Y.-H. Lee, D.-S. Moon, S.-C. Yoon, and J. C. Raymond, *Science* **342**, 6164 (2013).
- [3] N. Svendenius, *Phys. Scr.* **22**, 240 (1980).
- [4] N. Svendenius and J. Vergés, *Phys. Scr.* **22**, 288 (1980).
- [5] W. C. Martin, R. Zalubas, and A. Musgrove, *J. Phys. Chem. Ref. Data* **14**, 751 (1985).
- [6] S. N. Nahar, E. M. Hernández, L. Hernández, A. Antillón, A. Morales-Moric, O. González, A. M. Convington, K. C. Chartkunchand, D. Hanstorp, A. M. Juárez, and G. Hinojosa, *J. Quan. Spec. Rad. Tran.* **187**, 215 (2017).
- [7] E. Biémont, Y. Frémat, and P. Quinet, *At. Data Nucl. Data Tables* **71**, 117 (1999).
- [8] M. J. Vilkas and Y. Ishikawa, *J. Phys. B: At. Mol. Opt. Phys.* **37**, 4763 (2004).
- [9] P. Andersson, A. O. Lindahl, C. Alfredsson, L. Rogström, C. Diehl, D. J. Pegg, and D. Hanstorp, *J. Phys. B: At. Mol. Opt. Phys.* **40**, 4097 (2007).
- [10] R. J. Peláez, C. Blondel, M. Vandevraye, C. Drag, and C. Delsart, *J. Phys. B: At. Mol. Opt. Phys.* **44**, 195009 (2011).
- [11] D. E. Woon and T. H. Dunning, Jr., *J. Chem. Phys.* **99**, 3730 (1993).
- [12] C. Guo-xin, P. P. Ong, and L. Ting, *Chem. Phys. Lett.* **290**, 211 (1998).
- [13] G. L. Gutsev, P. Jena, and R. J. Bartlett, *Chem. Phys. Lett.* **291**, 547 (1998).
- [14] W. P. Wijesundera and F. A. Parpia, *Phys. Rev. A* **57**, 3462 (1998).
- [15] G. de Oliveira, J. M. L. Martin, F. de Proft, and P. Geerlings, *Phys. Rev. A* **60**, 1034 (1999).
- [16] C. F. Bunge, M. Galán, R. Jáuregui, and A. V. Bunge, *Nucl. Instr. Meth.* **202**, 299 (1982).
- [17] C. F. Bunge, *Phys. Rev. Lett.* **44**, 1450 (1980).
- [18] C. F. Bunge, *Phys. Rev. A* **22**, 1 (1980).
- [19] S. Mannervik, G. Astner, and M. Kisielinski, *J. Phys. B: At. Mol. Opt. Phys.* **13**, L441 (1980).
- [20] R. L. Brooks, J. E. Hardis, H. G. Berry, L. J. Curtis, K. T. Cheng, and W. Ray, *Phys. Rev. Lett.* **45**, 1318 (1980).
- [21] A. Denis and J. Desesquelles, *J. Physique Lett.* **42**, 59 (1981).
- [22] G. W. F. Drake, *Astrophys. J.* **189**, 161 (1973).
- [23] C. A. Nicolaidis, Y. Komninos, and D. R. Beck, *Phys. Rev. A* **24**, 1103 (1981).
- [24] V. L. Jacobs, A. K. Bhatia, and A. Temkin, *Astrophys. J.* **191**, 785 (1974).
- [25] P. O. Löwdon, *Rev. Mod. Phys.* **36**, 966 (1964).
- [26] A. V. Bunge, C. F. Bunge, R. Jáuregui, and G. Cisneros, *Comp. Chem.* **13**, 201 (1989).
- [27] R. Jáuregui, C. F. Bunge, A. V. Bunge, and G. Cisneros, *Comp. Chem.* **13**, 223 (1989).
- [28] A. V. Bunge, C. F. Bunge, R. Jáuregui, and G. Cisneros, *Comp. Chem.* **13**, 239 (1989).
- [29] C. X. Almora-Díaz, A. Ramírez-Solís, and C. F. Bunge, *Phys. Chem. Chem. Phys.* **21**, 4953 (2019).
- [30] O. Jitrik and C. F. Bunge, *Phys. Rev. A* **56**, 2614 (1997).
- [31] C. F. Bunge, *J. Chem. Phys.* **125**, 014107 (2006).
- [32] Available upon request from bunge@fisica.unam.mx.
- [33] C. F. Bunge and R. Carbó-Dorca, *J. Chem. Phys.* **125**, 014108 (2006).
- [34] C. X. Almora-Díaz, H. Rivera-Arrieta, and C. Bunge, *Adv. Quant. Chem.* **72**, 129 (2016).
- [35] C. F. Bunge, J. A. Barrientos, and A. V. Bunge, *At. Data Nucl. Data Tables* **53**, 113 (1993).
- [36] A. V. Bunge, *J. Chem. Phys.* **53**, 20 (1970).
- [37] C. Schwartz, *Phys. Rev.* **126**, 1015 (1962).
- [38] C. F. Bunge, R. Jáuregui, and E. Ley-Koo, *Can. J. Phys.* **76**, 421 (1998).
- [39] C. F. Bunge, E. Ley-Koo, and R. Jáuregui, *Mol. Phys.* **98**, 1067 (2000).
- [40] E. Ley-Koo, C. F. Bunge, and R. Jáuregui, *J. Mol. Struct.* **527**, 11 (2000).
- [41] R. Jáuregui, C. F. Bunge and E. Ley-Koo, *Phys. Rev. A* **55**, 1781 (1997).
- [42] G. E. Brown and D. G. Ravenhall, *Proc. Roy. Soc. London* **A208**, 552 (1951).
- [43] J. Sucher, *Phys. Rev. A* **22**, 348 (1980).
- [44] J. K. L. McDonald, *Phys. Rev.* **43**, 830 (1933).
- [45] C. F. Fischer, *Comput. Phys. Commun.* **14**, 145 (1978).
- [46] T. Koga, H. Aoki, J. M. Garcia de la Vega, and H. Tatewaki, *Theor. Chem. Acc.* **96**, 248 (1997).